

Structural, Dielectric, and Rheological Characterization of Thermotropic Liquid Crystalline Copolyesters Based on 4-Hydroxybenzoic Acid, 4,4'-Dihydroxybiphenyl, Terephthalic Acid, and Isophthalic Acid

Douglass S. Kalika,¹ Do Y. Yoon,* Pio Iannelli,² and William Parrish

IBM Almaden Research Center, 650 Harry Road, San Jose, California 95120

Received May 11, 1990; Revised Manuscript Received October 4, 1990

ABSTRACT: We have investigated the structures, segmental dynamics, and flow characteristics of two aromatic copolyesters: Xydar SRT-300 (Dartco) comprising 4-hydroxybenzoic acid (HBA), 4,4'-dihydroxybiphenyl (BP), and terephthalic acid (TA) in a 68/16/16 molar ratio and POB S6635 (Sumitomo) comprising HBA, BP, TA, and a small fraction of isophthalic acid (IA) "kinks" in a 62/19/15/4 ratio. The X-ray powder diffraction measurements indicate the predominance of a high degree of three-dimensional order in the annealed Xydar polymer, with a substantial reduction in the degree of order upon the introduction of a small fraction of kinked comonomer units in the POB polymer. At high temperatures below the transition to nematic melts, both polymers display one sharp X-ray peak characteristic of hexagonal interchain packing order of highly extended chains. The dielectric relaxation results show that the rotational motions of HBA dipoles are as active in the highly (three-dimensionally) ordered annealed Xydar samples as they are in less ordered quenched material. Both Xydar and POB polymers display a low-temperature Arrhenius-type (β) relaxation (ca. 0 °C for Xydar (10 kHz)) which corresponds to localized motions of the HBA dipoles, with the POB copolymer displaying an additional weak WLF-type (α) relaxation at higher temperatures (ca. 140 °C (10 kHz)). The measured relaxation strength for Xydar is much smaller than that of POB and indicates a high degree of conformational order that tends to cancel the dipole vectors of mobile ester groups, in close resemblance to the situation observed for the HBA homopolymer (PHBA) in the smectic E-type structure above 340 °C. In contrast to the Xydar result, the much larger relaxation strength observed for POB across the β transition indicates the absence of such conformational order, the dielectric increment approaching that expected for independent, uncorrelated reorientations of the HBA dipoles. Dynamic rheological measurements, limited to the POB polymer, indicate a shear-independent complex viscosity at low frequencies for the melt (370 °C) which is unusual for a nematic melt. Moreover, rheological cooling sweeps exhibit an essentially temperature-independent solidlike behavior throughout the temperature range 350 to 50 °C which appears to be dominated by the rudimentary interchain packing order but completely unaffected by the rapid rotational segmental motions.

Introduction

Since the initial development of poly(4-hydroxybenzoic acid) (PHBA) and subsequent recognition of its outstanding high-temperature properties, a number of hydroxybenzoic acid based copolyesters have been introduced in an attempt to combine these outstanding high-temperature characteristics with an ease of processability.³ The result has been a variety of commercial materials that display liquid crystalline characteristics in the melt, with processing temperatures ranging from approximately 250 °C to nearly 450 °C. Specifically, these copolymers have combined 4-hydroxybenzoic acid with comonomers of biphenol terephthalate (BPT, Carborundum),⁴ ethylene terephthalate (ET, Tennessee Eastman),⁵ and 6-hydroxy-2-naphthoic acid (HNA, Celanese).⁶ The work to be presented here is concerned with the first of these copolymer formulations and is comprised of structural, dielectric, and rheological characterizations of two commercial resins based on (1) 4-hydroxybenzoic acid (HBA), 4,4'-dihydroxybiphenyl (BP), and terephthalic acid (TA) [Xydar SRT-300, Dartco], and (2) HBA, BP, TA, and a small fraction of isophthalic acid (IA) [POB S6635, Sumitomo]. While these two polymers are compositionally very similar, the introduction of the meta-connected isophthalic acid monomer in POB S6635 has a significant effect on the polymer properties, since the introduction of such "kinks" prevents the long linear extended-chain conformations, which will in turn cause significant changes in the interchain packing order. The results obtained for these two materials will be discussed with an emphasis on

the influence of this chemical modification on the molecular order (as established by X-ray diffractometry), the rotational segmental dynamics (by dielectric spectroscopy), and the translational flow characteristics (by torsional rheometry).

Background

X-ray Diffraction. Wide-angle X-ray diffraction results on copolymers composed of HBA, BP, and TA indicate a high degree of axial orientation and three-dimensional order.⁷⁻⁹ Studies by Field and co-workers⁸ on a sample of composition 50/25/25 HBA/BP/TA reveal a polymorphic structure for the polymer, which is highly sensitive to thermal history. Specifically, for the as-synthesized material they report a crystal-crystal transition upon heating above 100 °C (from crystal form A to crystal form B) which is reversible upon cooling as long as the sample is not heated above the crystal-to-nematic transition temperature. If the material is quenched from the melt, however, subsequent heating sweeps reveal the absence of the crystal-crystal transition, with the resulting diffraction patterns indicative of a somewhat disordered B phase; this quenched form has been designated B(q). The (room temperature) A form can only be recovered by annealing the polymer above 260 °C, at which temperature the B(q) form is transformed to the B form; slow cooling through the crystal-crystal transition then provides the A form. (However, the three-dimensional ordered structures of these copolymers should be distinguished from the conventional crystals, as noted previously by Bechtoldt et al. for a copolyester comprising HBA/hy-

droquinone (HQ)/carbonate (CB)/BP/TA,¹⁰ since the HBA dipoles undergo rapid rotational motions even in the very highly ordered Xydar samples; see below.)

Dielectric Relaxation Measurements. Dielectric relaxation results, while not detailed for the HBA/BPT copolymers prior to this work, have been reported for the HBA/HNA copolymers^{11–14} and other HBA copolymers^{10,12,15} as well as for the PHBA homopolymer.¹⁴ In the previous paper, Kalika and Yoon¹⁴ describe the relaxations observed for HBA/HNA copolymers of varying composition; a sub-glass relaxation is observed at low temperatures with a dielectric increment that correlates directly with the HBA content of the copolymer, and a combined secondary transition and glass transition is observed at higher temperatures which is less sensitive to copolymer composition; measurements by Alhaj-Mohammed et al.¹³ recorded over a somewhat lower frequency range indicate two separate relaxations at higher temperatures for these materials which correspond to localized motions of the HNA segments and a very weak glass transition, respectively. Results for the HBA/ET copolymers reported by Gedde and co-workers¹⁵ indicate a localized sub-glass relaxation process and two separate glass transitions for the 60/40 HBA/ET copolymer, according to the peak temperatures in dielectric loss vs frequency in the 1 Hz to 100 kHz range; the 80/20 HBA/ET material displays only a single glass transition. Multiple glass transitions are not surprising for the 60/40 HBA/ET formulation as both proton NMR¹⁶ and rheological studies¹⁷ indicate that the material is biphasic at this composition. For a polymer comprising HBA/HQ/CB/BP/TA, Bechtoldt et al. observed a very strong sub-glass relaxation and a very weak glass transition peak.¹⁰ Moreover, they reported that the dielectric relaxation characteristics of this polymer were nearly independent of the extent of the three-dimensional order that could vary significantly depending on thermal history.

Rheology. As a result of the high level of commercial interest noted above and the relatively large quantities of resin available, a number of rheological studies have appeared that characterize the melt flow properties of the HBA-based thermotropic liquid crystalline copolymers. The rheological behavior of these materials tends to be very complex, as they are highly sensitive to mechanical and thermal history. One of the most fundamental questions with regards to liquid crystalline polymer rheology is the relationship between the observed viscosity-shear rate behavior and the microstructure of the material. Asada and Onogi¹⁸ developed a "three-region" viscosity-shear rate flow curve model based on observations of lyotropic (solution-based) liquid crystalline polymers which display three distinct regions of flow behavior with increasing shear rate: a steeply shear-thinning region at very low rates (region I), a shear-independent "plateau region" at intermediate rates (region II), and a second shear-thinning region at high rates (region III). These observations were confirmed by Wissbrun¹⁹ in the course of his review of existing data for various liquid crystalline polymer systems. The low shear rate range is of greatest interest, as the nearly yieldlike behavior appears to be closely related to the polydomain texture that is observed optically in quiescent samples. Specifically, Asada and Onogi identify the onset of region II (shear-independent) flow behavior with the ultimate coalescence of polydomains into a monodomain texture.

While the existence of three-region flow behavior has been reported for a number of lyotropic liquid crystalline systems over a wide range of shear rates,¹⁹ three-region

behavior has not been convincingly demonstrated for thermotropic systems, in which the polydomain texture appears to persist to higher rates. Steady shear viscosity measurements on the 80/20 HBA/ET copolymer over eight decades of shear rate indicate a persistent shear-thinning behavior, with no shear-independent region;²⁰ similar behavior has been observed for the 60/40 HBA/ET copolymer,^{21,22} although there is a hint of a shear-independent plateau at rates above 10^4 s⁻¹. Capillary experiments on the 73/27 HBA/HNA copolyester also reveal a high degree of shear thinning,^{23,24} with data by Wissbrun²³ again suggesting a possible shear-independent viscosity above 10^4 s⁻¹. Dynamic rheological measurements on these copolymers typically fail to reveal a plateau viscosity over the frequency range of 0.1–100 rad/s.^{17,20,23–25}

In the work described below, dynamic rheological studies were performed on the POB S6635 copolymer in order to further expand the available information on the viscosity-shear rate behavior of these thermotropic materials. Unfortunately, rheological measurements could not be carried out for the Xydar resin, as the necessary test temperature is beyond the range of our rheological equipment.

Experimental Methods

Material Properties. The Xydar SRT-300 resin was obtained from Dartco Manufacturing Inc., while the POB S6635 (formerly Ekonol E6000) sample was obtained through the courtesy of Sumitomo Chemical America; both polymers were supplied in the form of pellets. ¹H NMR measurements on hydrolized samples of the two materials by Niessner and co-workers²⁶ indicate the following compositions: Xydar SRT-300, 68 (mol %) HBA/16% BP/16% TA; POB S6635, 62% HBA/19% BP/15% TA/4% IA. Differential scanning calorimetry (DSC) studies on the as-received Xydar samples show a broad melting endotherm at approximately 410 °C (at 20–50 °C/min heating rate), while the DSC sweeps for the POB resin display no distinct transitions. The technical literature accompanying the Xydar material report a DSC melting transition of 421 °C,²⁷ and the POB processing range is reported to be 330–350 °C.²⁸ Rheological measurements performed in the course of this work place the flow temperature of the POB polymer at just below 360 °C; both materials are reported to exhibit liquid crystalline melts above their respective flow temperatures.^{27,28} Thermogravimetric analysis (TGA) on the polymers indicates thermal stability up to 400 °C.

X-ray Diffraction. The X-ray diffraction apparatus and data-handling methods employed in this work have been detailed previously.^{29,30} Pellets of both polymers were ground at sub-ambient temperature, and the X-ray powder samples were prepared on thin silicon single-crystal wafers using silicone grease as a binder. Initial (room temperature) diffraction patterns were recorded over the range 5–55° (2 θ), with subsequent patterns typically spanning 10–35°; the step increment was 0.05° (2 θ). Patterns were recorded over various thermal histories at temperatures ranging to 420 °C for POB and to 460 °C for Xydar.

Dielectric Relaxation Measurements. The dielectric relaxation characteristics of the two materials were established by measurement of the dielectric constant (ϵ') and loss (ϵ'') under an inert atmosphere at temperatures ranging from –100 to 225 °C; all measurements were recorded at a heating rate of 10 °C/min. A frequency range of 0.4 kHz to 4 MHz was accomplished by combination of the Hewlett-Packard multifrequency LCR meter Models 4274A and 4275A. Dielectric test samples were prepared by pressing individual resin pellets at flow temperature between glass slides upon which gold electrodes had been previously evaporated; the electrode diameter was 11 mm. Typical sample thicknesses were 0.1 mm for POB and 0.3 mm for Xydar (for additional details, see the previous paper¹⁴). In order to achieve consistent results, it was necessary to dry the resin pellets under vacuum for 24 h (120 °C) prior to sample preparation. In order to cover the full frequency range offered by the two HP LCR meters, two successive heating sweeps were required. Over the temperature range of investigation employed for the copolymers, the dielectric data showed no influence of

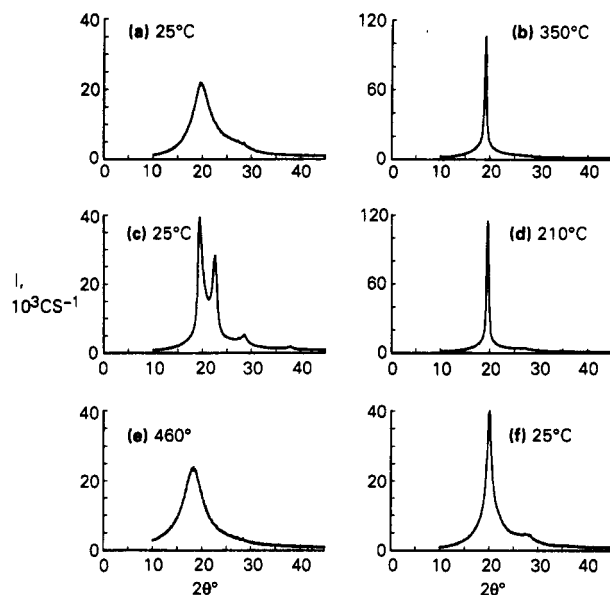


Figure 1. X-ray diffraction results (intensity (counts/s) versus $2\theta^\circ$) for Xydar SRT-300: (a) 25 °C, as-received sample; (b) 350 °C (note change in intensity scale); (c) 25 °C, after annealing at 350 °C; (d) 210 °C (note scale); (e) 460 °C; (f) 25 °C, after cycling to 460 °C.

annealing. Five test samples were prepared for each polymer, and the reproducibility of the measured dielectric parameters was evaluated at room temperature; the values of dielectric constant and loss were found to be in agreement for the various samples within $\pm 2\%$.

Rheology. Dynamic rheological measurements were performed with a Rheometrics mechanical spectrometer Model 705 equipped with a 2000 g-cm torque transducer; both the parallel-plate and cone-and-plate geometries were used (25-mm platens, cone angle of 0.1 rad). Owing to the extreme flow temperature of the Xydar resin, only the POB polymer was investigated. Samples were held under vacuum for a minimum of 24 h (120 °C) prior to measurement in order to remove moisture and loaded into the rheometer in pellet form at the test temperature under a nitrogen atmosphere. Constant-temperature frequency sweeps were recorded at 370 °C over a frequency range of 0.1–100 rad/s; both ascending and descending frequency progressions were performed at strain amplitudes of 10–100%. In addition, the dynamic rheological parameters of the polymer were recorded over a cooling history for samples loaded at 370 °C. Serrated parallel platens were employed for the cooling sweeps in order to minimize the possibility of sample slippage at temperatures below the solidification point.

Results

X-ray Diffraction. The X-ray diffraction pattern recorded for the as-received Xydar SRT-300 resin is shown in Figure 1a: it features a broad asymmetric peak with maximum at 19.72° (2θ , $d = 4.50$ Å). Upon heating directly to 350 °C and annealing for 1 h, the central peak sharpens and shifts to 19.10° ($d = 4.65$ Å) with a considerable increase in intensity (Figure 1b, note change in intensity scale). Upon cooling to 25 °C, a highly ordered pattern evolves, with reflections at 19.48° (4.55 Å), 22.58° (3.94 Å), 28.60° (3.12 Å), and 37.96° (2.37 Å, Figure 1c). These features are nearly identical with those reported by Field *et al.*⁸ for an as-synthesized sample (and a sample cooled slowly from 380 °C) composed of 50/25/25 HBA/BP/TA. Subsequent heating to 460 °C produces an amorphous pattern centered at 18.36° (4.83 Å, Figure 1e), and upon returning to room temperature, the effects of the prior annealing history are seen to be virtually erased (Figure 1f), with the final pattern appearing as a sharper form of the original as-received result, with peaks at 19.7° and ca.

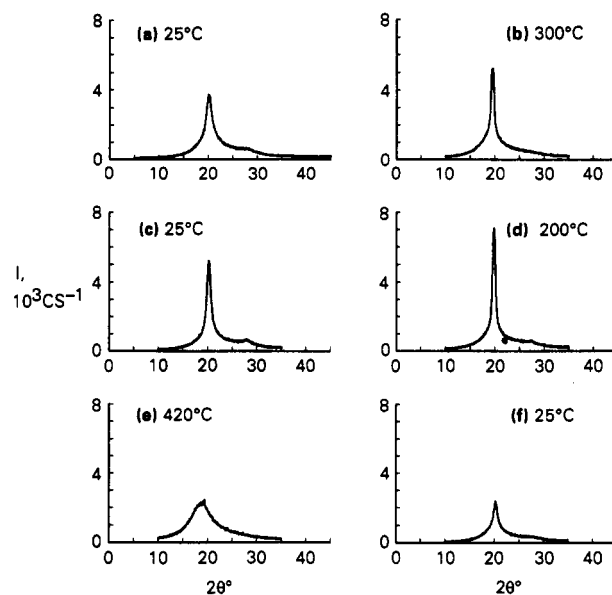


Figure 2. X-ray diffraction results (intensity (counts/s) versus $2\theta^\circ$) for POB S6635: (a) 25 °C, as-received sample; (b) 300 °C; (c) 25 °C, after cycling to 300 °C; (d) 200 °C; (e) 420 °C; (f) 25 °C, after cycling to 420 °C.

28° (2θ), respectively. Our X-ray measurements for the SRT-300 resin as a function of thermal history agree very closely with the results reported by Field and co-workers,⁸ and hence no additional Xydar diffraction results will be detailed here.

X-ray diffraction results recorded for the POB S6635 copolymer do not show the high sensitivity to thermal history and annealing that was evident for the Xydar material. X-ray-temperature patterns analogous to those described above are provided in Figure 2: the as-received material was initially heated to 300 °C with patterns recorded at numerous intervals, cooled to room temperature, and then cycled to 420 °C. Although specific long-time annealing was not imposed on the sample, it was necessary to hold the material for approximately 20 min at each temperature in order to record a full diffraction pattern. The room temperature result for the as-received POB S6635 (Figure 2a) is very similar to that observed for the Xydar resin, but cycling to 300 °C does not produce the high degree of order that was evident after annealing the Xydar SRT-300. Comparison of the POB patterns recorded before and after this first heating cycle (refer to Figure 2) shows a sharpening of the features, the annealed polymer displaying reflections at 20.25° (4.38 Å) and 27.95° (3.19 Å), but no additional peaks. Upon incremental heating to 420 °C, these features are eventually removed (Figure 2e), and subsequent cooling produces a pattern similar to the as-received result (Figure 2f). A full three-dimensional intensity/ $2\theta^\circ$ /temperature plot for this second heating cycle is provided in Figure 3. The strong peak at approximately 20° (110/200 reflection; see below) sharpens and increases in intensity with increasing temperature, and the d spacing shifts to higher values due to thermal expansion (Figure 4); no distinct phase transition is evident in the d -spacing results. At 180 °C the intensity of this reflection reaches a maximum, and the pattern is essentially reduced to an amorphous halo by 420 °C. The weak reflection at approximately 28° (211 reflection; see below) decreases in intensity with temperature throughout the range, disappears by 300 °C, and does not reappear upon cooling from the nematic melt. As is evident from the intensity and d -spacing results (Figure 4), however, the X-ray patterns are completely reversible (after the first heating) for thermal cycles up to at least 300 °C.

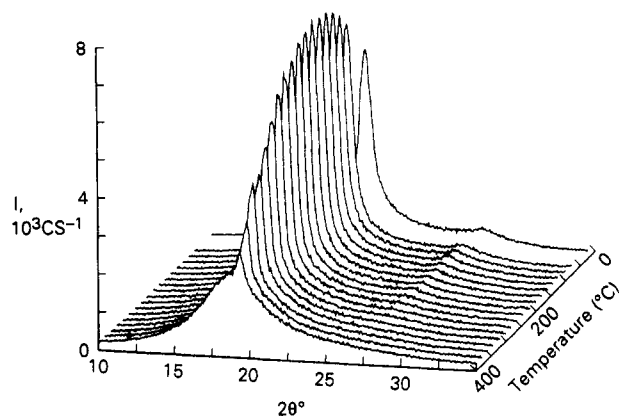


Figure 3. X-ray diffraction results for POB S6635: intensity (counts/s) versus $2\theta^\circ$ versus temperature ($^\circ\text{C}$) for second heating cycle.

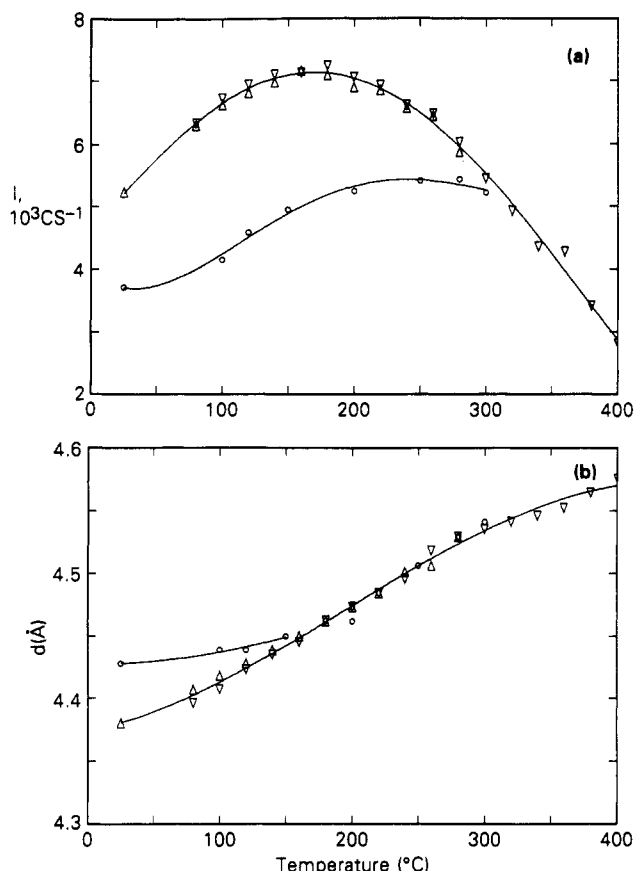


Figure 4. X-ray diffraction results for the 110/200 reflection of POB S6635: (a) intensity (counts/s) versus temperature ($^\circ\text{C}$); (b) d spacing (\AA) versus temperature ($^\circ\text{C}$). (○) First heating (to 300°C); (Δ) cooling; (▽) second heating.

Dielectric Relaxation Measurements. The dielectric characteristics of the two polyesters are provided as plots of dielectric constant (ϵ') and loss (ϵ'') versus temperature for the various frequencies investigated (Figures 5 and 6). Initial examination of these data reveals a strong relaxation over the range -100 to $+150^\circ\text{C}$, with the relaxation strength significantly greater for the POB S6635 material; the dielectric loss curves display a single distinct maximum for each case, with a sharp increase in ϵ'' at higher temperatures due to the onset of ionic conduction. This ionic conduction contribution can be effectively removed from the measured dielectric loss data by the method described previously;¹⁴ in the present case, the conduction contribution frequency exponent (a , $\epsilon'' \rightarrow \omega^a$) has a value of -0.65 for both polymers. The conduction-corrected di-

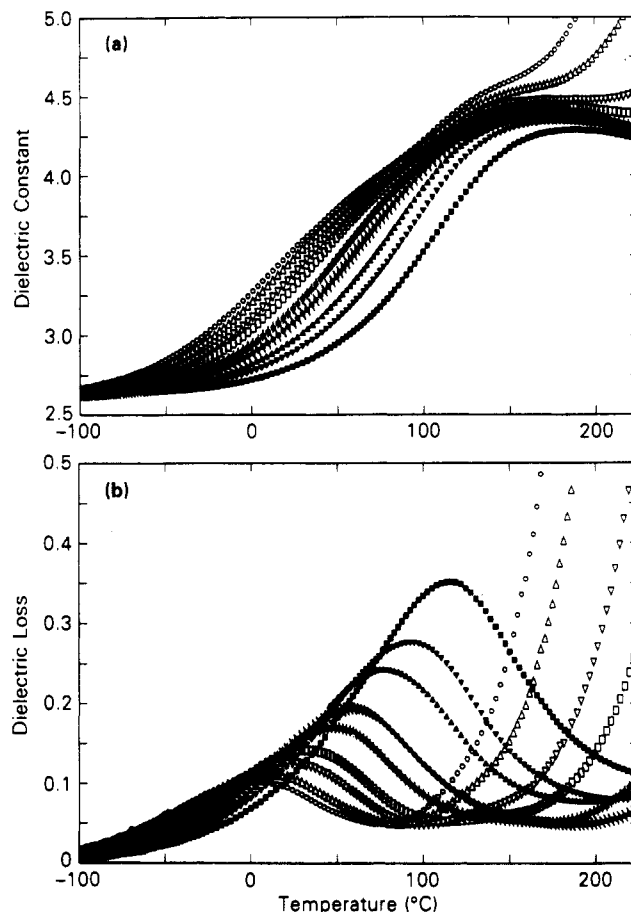


Figure 5. Dielectric results for POB S6635, recorded at $+10^\circ\text{C}/\text{min}$: (a) dielectric constant (ϵ') versus temperature ($^\circ\text{C}$); (b) dielectric loss (ϵ'') versus temperature ($^\circ\text{C}$). (○) 0.4 kHz; (Δ) 1 kHz; (▽) 4 kHz; (□) 10 kHz; (Φ) 40 kHz; (⊗) 100 kHz; (▲) 0.4 MHz; (▼) 1 MHz; (■) 4 MHz.

electric loss curves for the POB and Xydar polymers at all frequencies investigated are provided in Figure 7. Examination of the (conduction-corrected) POB loss data reveals a second, weaker relaxation at higher temperatures; this relaxation is not evident in the Xydar results.

Constant-temperature Argand plots (ϵ'' versus ϵ') in the range of the low-temperature relaxation process are shown in Figure 8 (POB S6635, selected temperatures) and 9 (Xydar SRT-300). The symmetric data can be described by application of the Cole-Cole equation

$$\epsilon^* = (\epsilon_r - \epsilon_u) / (1 + (i\omega\tau)^\beta) \quad (1)$$

where ϵ^* , the complex dielectric constant, is related to the relaxed and unrelaxed values of the dielectric constant (ϵ_r , ϵ_u), the frequency (ω), a central relaxation time (τ), and a symmetric broadening parameter (β); the semicircular arcs in Figures 8 and 9 represent least-squares fits to the Cole-Cole equation. The unrelaxed dielectric constant (ϵ_u) is found to be independent of temperature for both polymers, but the relaxed dielectric constant (ϵ_r) shows a linear temperature dependence that is very strong for the POB case (Figure 10). The broadening parameter (β) is also a strong function of temperature (Figure 11a) and can be fit to an exponential expression

$$\beta/\beta_0 = \exp\{A(T - T_0)\} \quad (2)$$

Combination of the ϵ_u , ϵ_r , and β values obtained from each Argand equation diagram allows the determination of the central relaxation time (τ , Figure 11b) from eq 1, and these

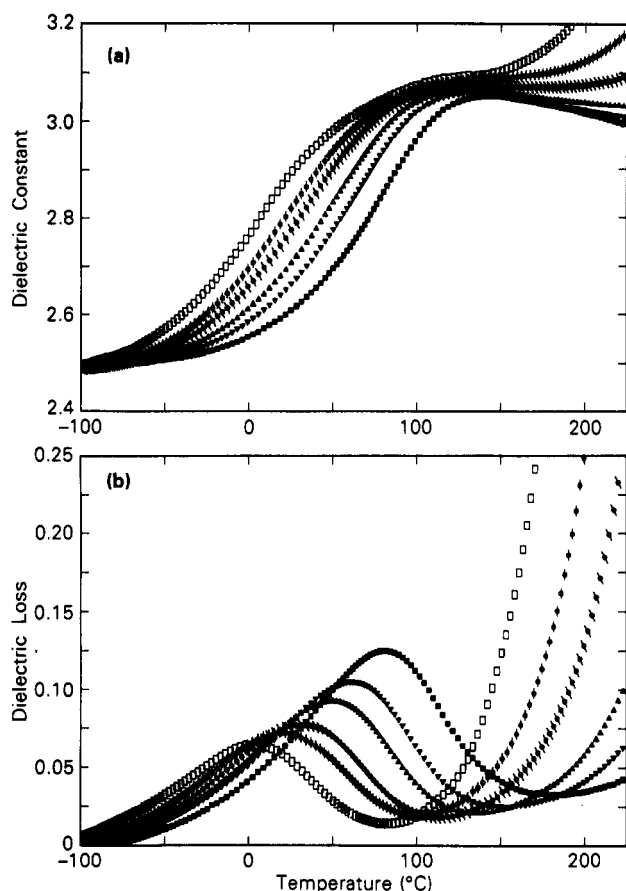


Figure 6. Dielectric results for Xydar SRT-300 recorded at +10 °C/min: (a) dielectric constant (ϵ') versus temperature (°C); (b) dielectric loss (ϵ'') versus temperature (°C). (\square) 10 kHz; (\diamond) 40 kHz; (\circ) 100 kHz; (\blacktriangle) 0.4 MHz; (\blacktriangledown) 1 MHz; (\blacksquare) 4 MHz.

data also follow the Arrhenius relation

$$\tau/\tau_0 = \exp(H/RT) \quad (3)$$

Introduction of the expressions for the various temperature-dependent Cole-Cole parameters into eq 1 provides a means for predicting the loss curves of the low-temperature relaxation across the entire temperature range (see POB result, Figure 12). This approach is particularly useful with regards to the (conduction-corrected) POB data, as it allows separation of the two overlapping loss processes (Figure 13). Arrhenius plots of frequency versus maximum temperature (isochronal basis) for the two separated POB relaxations and the single Xydar relaxation are shown in Figure 14. The low-temperature relaxations (designated as the β relaxation for both POB and Xydar) display a linear Arrhenius behavior, with activation energies of approximately 17 and 14 kcal/mol, respectively. The high-temperature POB relaxation (α relaxation) displays a nonlinear WLF-type behavior that can be described by

$$\log(\omega) = 27(T - T_0)/[85 + (T - T_0)] \quad (4)$$

with the reference temperature $T_0 = 95.8$ °C corresponding to a frequency of 1 Hz.

At this point a comment is necessary with respect to the influence of thermal history on the measured dielectric properties of the copolymers, given the observed influence of annealing on the structural characteristics of the Xydar material. For the case of the POB resin, the influence of thermal history can be assessed by comparing the dielectric results obtained at the overlapping frequencies (10, 40, and 100 kHz) for consecutive temperature sweeps

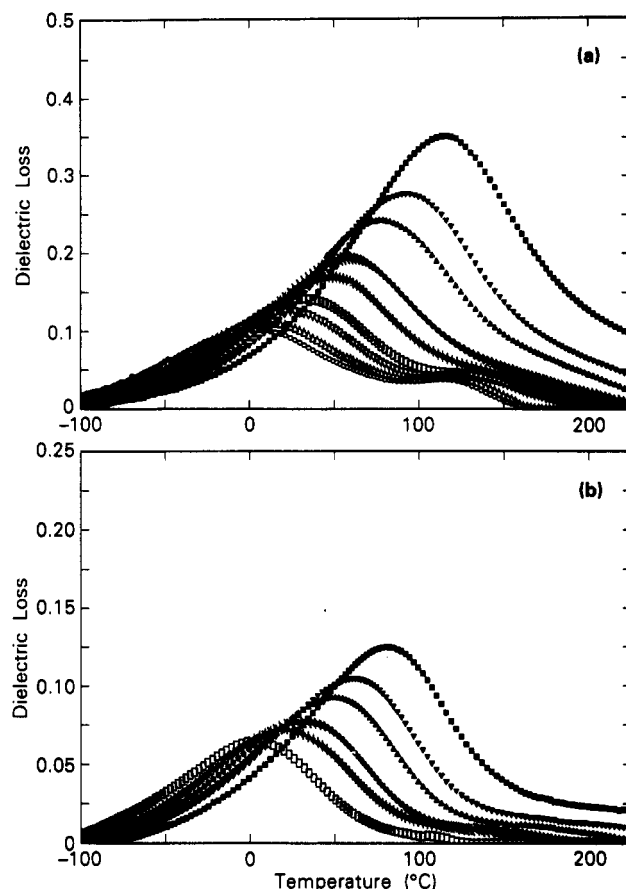


Figure 7. Dielectric loss data corrected for ionic conduction (0.4 kHz to 4 MHz): (a) POB S6635; (b) Xydar SRT-300. Symbol designations are the same as in Figure 5.

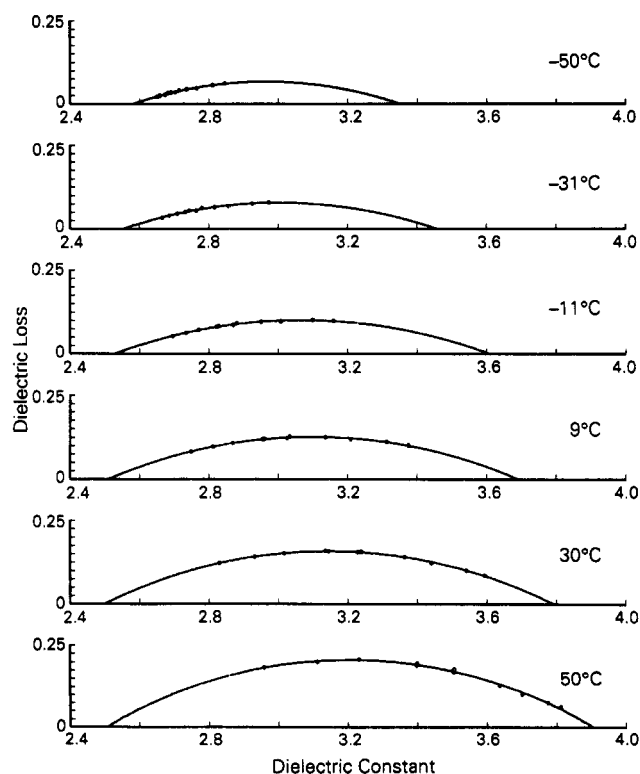


Figure 8. Selected Argand plots for POB S6635 at temperatures between -50 and +50 °C. Semicircular arcs represent the least-squares fits to the Cole-Cole equation.

using the HP LCR meter Models 4274A and 4275A, respectively. These sweeps were performed on thin, single-pellet samples that had been pressed from the melt at

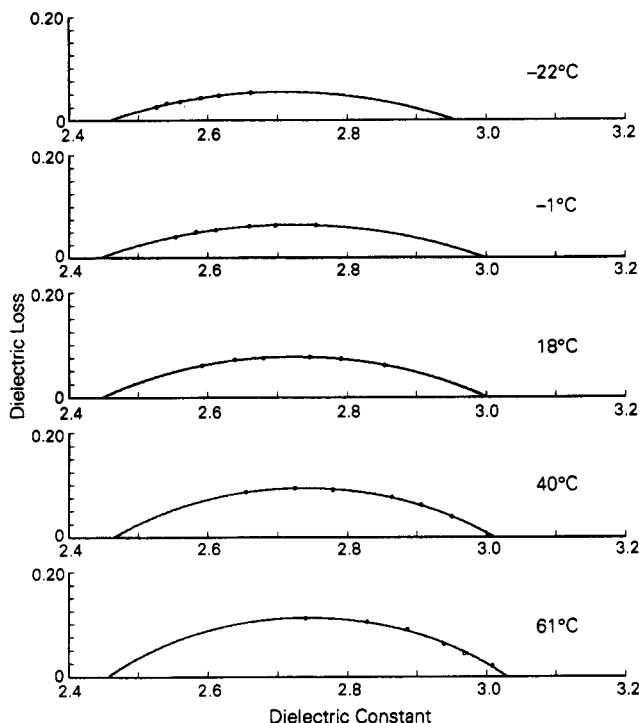


Figure 9. Argand plots for Xydar SRT-300 at temperatures between -22 and $+61$ $^{\circ}\text{C}$. Semicircular arcs represent the least-squares fits to the Cole-Cole equation.

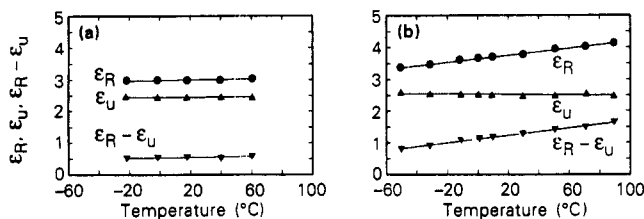


Figure 10. Relaxed and unrelaxed limits of the dielectric constant versus temperature ($^{\circ}\text{C}$) based on the Argand plots: (a) Xydar SRT-300; (b) POB S6635.

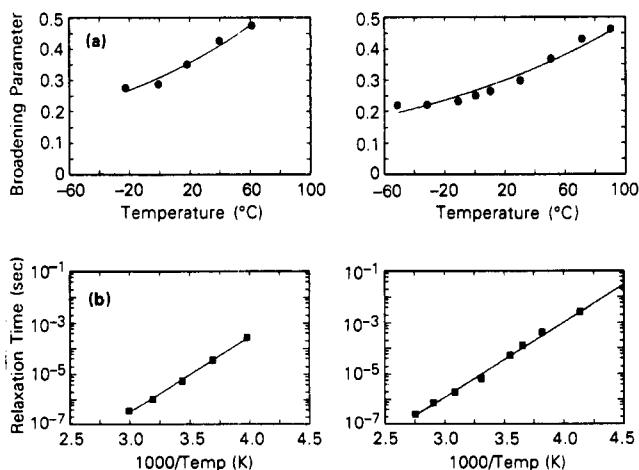


Figure 11. Cole-Cole parameters as a function of temperature for Xydar SRT-300 (left) and POB S6635 (right) based on the Argand plots: (a) Cole-Cole broadening parameter (β) versus temperature ($^{\circ}\text{C}$); (b) central relaxation time (τ , s) versus $1000/\text{temperature}$ (K).

approximately 370 $^{\circ}\text{C}$ and then quenched to room temperature. Multiple runs over the range -100 to $+225$ $^{\circ}\text{C}$ indicate no influence of thermal history or annealing on the POB dielectric results.

For the case of the Xydar resin, specific dielectric annealing experiments were performed under conditions

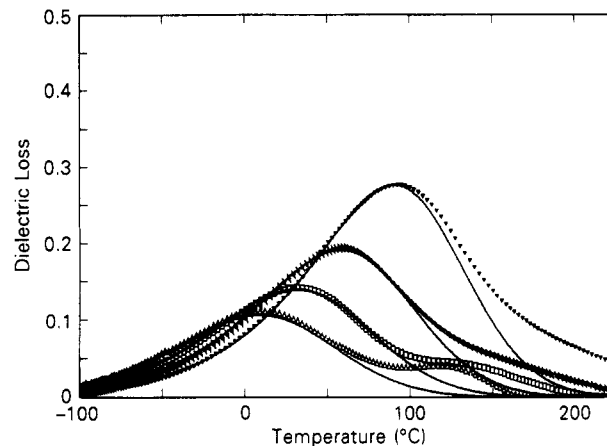


Figure 12. Dielectric loss data for POB S6635 (corrected for conduction) at selected frequencies (1, 10, 100 kHz; 1 MHz) versus temperature ($^{\circ}\text{C}$). Solid lines represent empirical curve fits based on Cole-Cole parameters.

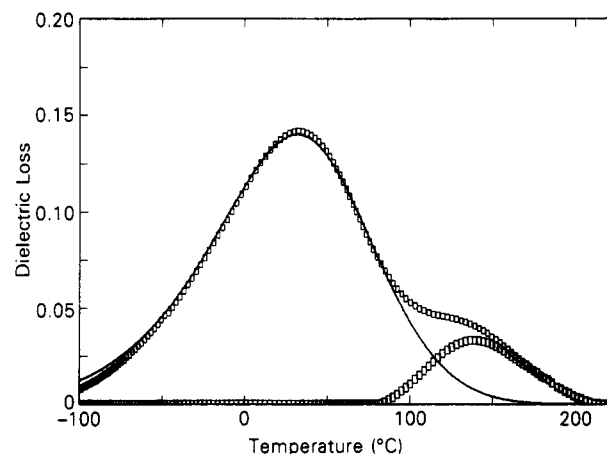


Figure 13. Dielectric loss for POB S6635 versus temperature ($^{\circ}\text{C}$) at 10 kHz. Solid line represents Cole-Cole based curve fit for low-temperature (β) relaxation; (\square) data for high-temperature (α) relaxation obtained by difference.

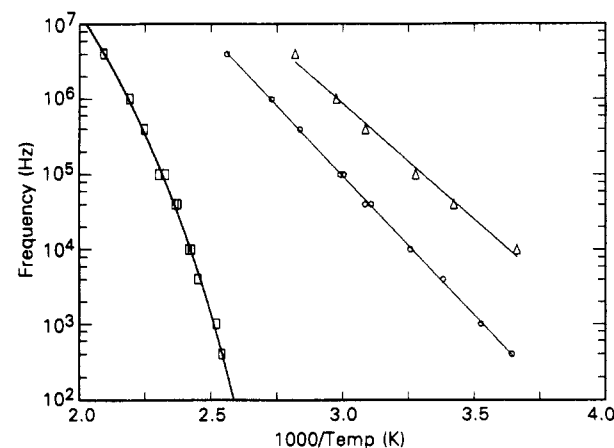


Figure 14. Arrhenius plot for POB S6635 and Xydar SRT-300 based on isochronal temperature sweeps. (\circ) POB, β relaxation; (Δ) Xydar, β relaxation; (\square) POB, α relaxation. Solid line represents WLF fit (see text).

similar to those employed for the X-ray diffractometry studies. In an effort to minimize the level of ionic conduction encountered at the high temperatures involved in these experiments, fused plaques 25 mm in diameter and 1.25 mm thick were compression molded from Xydar pellets at 430 $^{\circ}\text{C}$. While the increased thickness of the plaques reduces the observed level of conduction relative to the thin samples pressed from individual pellets, the

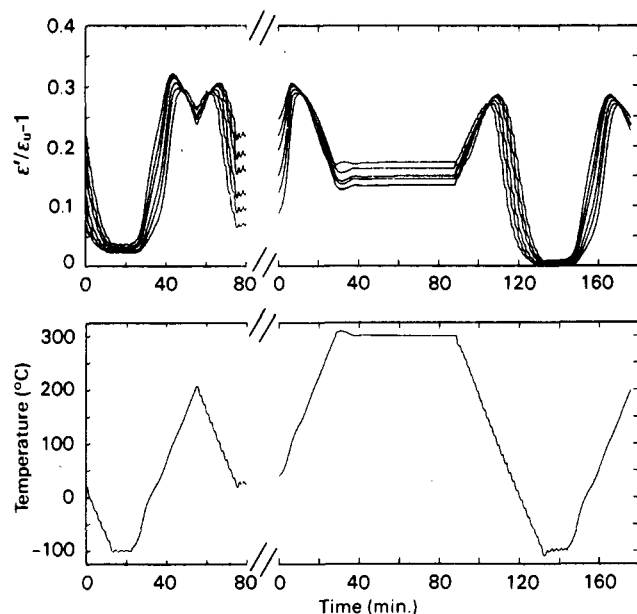


Figure 15. Dielectric constant (plotted as $\epsilon'/\epsilon_u - 1$) versus time (min) for Xydar SRT-300 subjected to the temperature cycling plotted in the lower diagram.

measured values of the dielectric constant for the plaques tend to be less reproducible and somewhat higher than those realized for the single pellet samples. The observed qualitative dielectric relaxation behavior for the two sample preparations is in agreement, however, and annealing of the plaque samples at 300 °C for 1 h appears to have no influence on the measured dielectric properties of the material. This result is demonstrated in Figure 15 for a plaque that was fused at 430 °C and cooled to room temperature over approximately 30 min: subsequent dielectric measurements (10 kHz to 4 MHz) were carried out for an initial temperature sweep from -100 to +200 °C (10 °C/min), an annealing period of 1 h at 300 °C, and a second temperature sweep from -100 to +200 °C. Examination of Figure 15, wherein the dielectric constant is plotted as $(\epsilon'/\epsilon_u - 1)$ versus time (ϵ_u determined at -100 °C, 4 MHz), reveals no net change in the measured dielectric increment for the relaxation at -100 to +150 °C over two cycles and no change in dielectric constant during the 1 h of annealing time at 300 °C. Hence, the rather significant changes in the interchain packing order with annealing that are indicated by the X-ray diffraction patterns have little influence on the local rotational segmental dynamics for either POB or Xydar. In other words, the local segmental rotations of HBA dipoles are as active in the highly ordered three-dimensional structures of these polymers as in the much less ordered quenched samples.

Rheology. As noted above, the rheological results for the POB S6635 resin are comprised primarily of dynamic frequency sweeps recorded at 370 °C. At this temperature, measurements of the complex melt viscosity as a function of time indicate that the material is stable over the time scale of the frequency sweeps (approximately 5 min), with the rheological parameters ($|\eta^*|$, G' , G'') remaining virtually unchanged. A typical (ascending) frequency sweep result (50% strain) is shown in Figure 16, with a total of four individual samples investigated; data recorded with the cone-and-plate geometry are indistinguishable from the parallel-plate results. The data display a "plateau" (frequency-independent) magnitude of the complex viscosity at lower frequencies, with shear-thinning behavior above 1 rad/s. Frequency sweeps

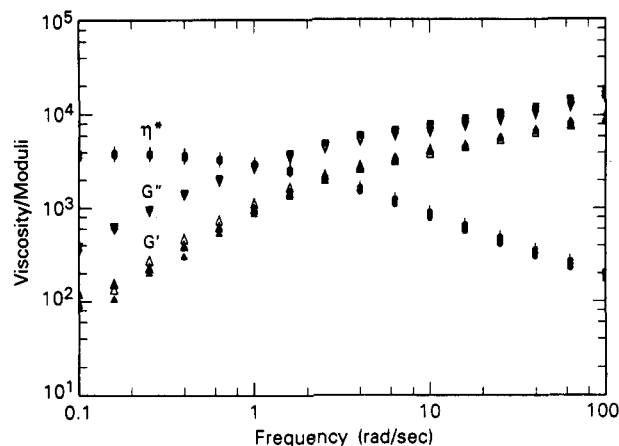


Figure 16. Dynamic rheological results for POB S6635: magnitude of the complex viscosity ($|\eta^*|$, P), storage modulus (G' , dyn/cm²), and loss modulus (G'' , dyn/cm²) versus frequency (rad/s); 370 °C, 50% strain. (○) $|\eta^*|$, (▲) G' , (▼) G'' (parallel plate); (○) $|\eta^*|$, (Δ) G' , (▽) G'' (cone and plate).

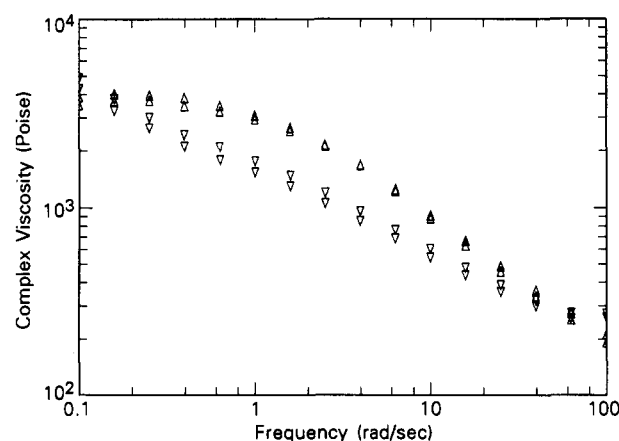


Figure 17. Dynamic rheological results for POB S6635: magnitude of the complex viscosity ($|\eta^*|$, P) versus frequency (rad/s); parallel-plate geometry, 50% strain, 370 °C. (Δ) Ascending frequency progression; (▽) descending frequency progression.

recorded in a descending manner (frequency progressing from 100 to 0.1 rad/s, 50% strain) are compared with the ascending sweeps in Figure 17. The magnitude of the complex viscosity is significantly reduced for the descending sweeps, particularly in the mid-frequency range, and no frequency-independent viscosity behavior is evident. Ascending sweeps recorded with various strain amplitudes (10%, 20%, 50%, 100%; 370 °C) are shown in Figure 18. The magnitude of the complex viscosity is essentially independent of strain amplitude at the lowest frequencies investigated, but at the higher frequencies the material is clearly nonlinear, the measured complex viscosity decreasing with increasing strain amplitude.

A temperature sweep for the POB S6635 is detailed in Figure 19; the material was loaded into the rheometer at 370 °C, with dynamic rheological parameters recorded directly over a cooling rate of 2 °C/min (1% strain). Above 350 °C, the material is fluid, with the loss modulus (G'') approximately 3 times greater than the storage modulus (G'). Upon cooling below 350 °C, solidification occurs, and both the storage and loss moduli increase sharply, the loss modulus displaying a maximum at 330 °C; below this temperature G' is more than an order of magnitude greater than G'' . At 275 °C, both moduli drop significantly and then remain nearly independent of temperature; the scatter in the loss modulus at these temperatures reflects the sensitivity limits of the rheometer at low loss angle.

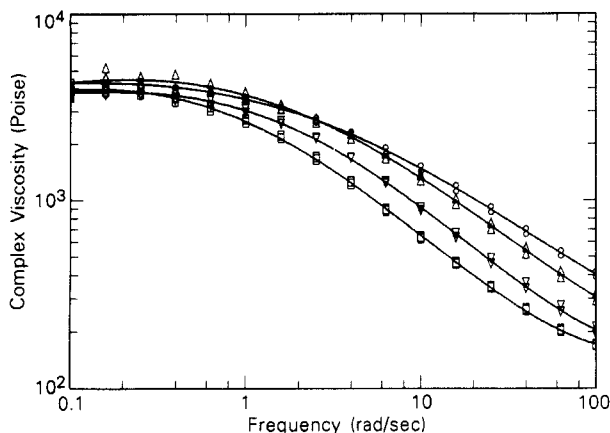


Figure 18. Dynamic rheological results for POB S6635: magnitude of the complex viscosity ($|\eta^*|$, P) versus frequency (rad/s) at varying strain amplitudes; parallel-plate geometry, 370 °C. (○) 10% strain; (Δ) 20% strain; (▽) 50% strain; (□) 100% strain.

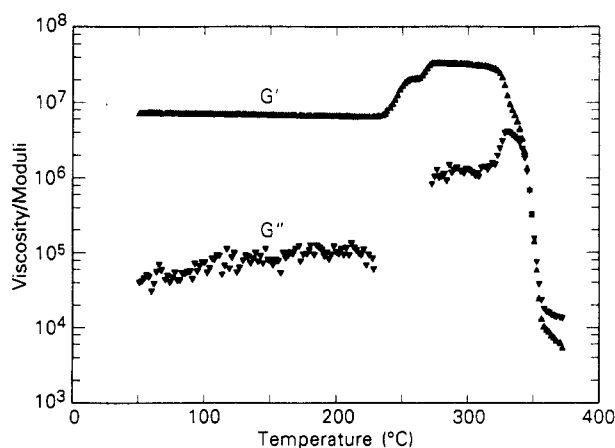


Figure 19. Dynamic rheological results for POB S6635: storage modulus (G' (Δ), dyn/cm²) and loss modulus (G'' (▽), dyn/cm²) versus temperature (°C) for cooling sweep initiated at 370 °C (2 °C/min); parallel-plate geometry, 1% strain, frequency = 10 rad/s.

Discussion

X-ray Diffraction. As is evident from the significantly lower processing temperatures encountered for the POB S6635 copolymer as compared to the Xydar SRT-300 resin, the introduction of a small fraction of isophthalic acid comonomer into the rigid, linear structure of the HBA/BPT formulation has a dramatic effect on material structure and properties. With respect to the X-ray diffraction results, it is readily obvious that the high degree of order that develops in the Xydar material upon annealing is not accomplished during cycling of the POB polymer. The first POB heating progression, in which the material is taken stepwise from room temperature to 300 °C and subsequently cooled, produces a sharper diffraction pattern than the initial (as-received) result (refer to Figure 2), but no new features evolve. The X-ray pattern with the two peaks at 20.25 and 27.95° (2θ) resembles that of PHBA above ca. 340 °C,³⁰⁻³² except that the sharp 00 l reflections of PHBA are missing and the 211 peak is much weaker in POB. The absence of 00 l peaks is consistent with the random copolymer structure, and taking $c = 12.55$ Å from the structure of PHBA,³⁰ the two peaks are indexed as 110/200 and 211, respectively, with an orthorhombic cell of $a = 8.76$ Å and $b = 5.06$ Å. At high temperatures above ca. 300 °C the X-ray results show only one remaining peak, which represents the (100) hexagonal interchain packing order; it decreases gradually in intensity

with temperature but does not disappear completely even at ca. 400 °C (see Figures 3 and 4).

The room temperature X-ray pattern obtained for a well-annealed Xydar sample displays three sharp peaks at 19.48, 22.58, and 28.60° (2θ) which can also be indexed as 110, 200, and 211 reflections of an orthorhombic cell with $a = 7.88$ Å and $b = 5.57$ Å (c being fixed at 12.55 Å from the PHBA structure). As first shown by Field et al.,⁸ the 110 and 200 peaks merge around 100 °C, with the X-ray pattern closely resembling that of POB at room temperature with a sharper 211 peak and hence PHBA above ca. 340 °C.³⁰⁻³² The 211 peak continues to decrease in intensity and disappears around ca. 300 °C. Upon further heating, the intensity and sharpness of the resultant hexagonal interchain (100) peak are maintained up to ca. 400 °C (see Figure 1b and reference 8). The dielectric measurements show, however, that the chain segments undergo rapid rotational motions even in the most highly ordered structures of Xydar; twofold 180° rotational jumps in the herringbone-type local structure of the aromatic moieties are most likely in close analogy to the situation of PHBA above ca. 340 °C.^{14,30}

Dielectric Relaxation Measurements. The dielectric relaxation measurements were carried out on samples that essentially represent the quenched form of the copolymers: sample films were pressed from the nematic melt and cooled rapidly to room temperature with no additional annealing. Multiple sweeps performed over the range -100 to +225 °C showed no influence of thermal history. The dominant, low-temperature transition (β transition) observed for both copolymers appears to correspond to localized motions of the HBA ester dipoles, as the measured activation energies and the location of the isochronal loss maxima are very close to those observed for both the poly-(4-hydroxybenzoic) acid homopolymer (PHBA) and the HBA/HNA copolymers.¹⁴ Estimation of the relative dipolar mobilities of the HBA groups across the β transition for both polymers can be accomplished by comparing with the prediction of the Onsager equation for the full, unhindered dipolar mobility (see the previous paper¹⁴); only the permanent dipolar components perpendicular to the polymer chains are considered, as relatively little translational contribution is expected. Comparing the values of the dielectric increment ($\Delta\epsilon = \epsilon_r - \epsilon_u$) calculated using an assumption of full, uncorrelated dipolar rotation with the observed experimental values, one finds that the fraction of "fully mobile" dipoles (measured dielectric increment normalized by calculated value) varies significantly with increasing temperature for the case of the POB resin. Across the range of the Argand plots, the fraction of "fully mobile" dipoles varies from 0.26 (-50 °C) to 0.87 (90 °C) for POB, while the values obtained for Xydar remain nearly independent of temperature (fraction of "fully mobile" dipoles ~ 0.25 , which is very close to the value obtained for PHBA at ca. 340 °C); these results directly reflect the temperature dependence of the quantity $\epsilon_r - \epsilon_u$ (see Figure 10). The value obtained for the fraction of "fully mobile" dipoles in the Xydar copolymer suggests that the local conformations of the HBA moieties are such that successive (mobile) HBA dipoles tend to cancel one another, the polymer chains approaching a 2₁ screw configuration along the chain axis, very much like the situation observed for the PHBA homopolymer in the smectic E type structure above ca. 340 °C and for the HBA/HNA copolyesters.¹⁴ In contrast to this result, the HBA moieties in POB apparently do not assume such ordered conformations, most likely owing to the presence of the kinked (isophthalic acid) comonomer units. In this regard, the

result for POB is very close to the previous finding of Bechtoldt et al. for the HBA/HQ/CB/BP/TA polymer, which also contains kinked carbonate comonomer units.¹⁰

At higher temperatures, an additional (α) relaxation is observed for the POB S6635 copolymer; this relaxation is not encountered with the Xydar material. The α relaxation, while much weaker than the β relaxation (see Figure 13), displays a higher activation energy, and the isochronal loss maxima can be satisfactorily described by a WLF-type fit. Given the absence of this loss in the Xydar results and its small relaxation strength, it is reasonable to assign the α relaxation to localized motions involving the "kinked" isophthalate segments, which would most likely require a larger degree of cooperation between chains, thus leading to the observed WLF-type behavior.

It should be noted here that there is no separate relaxation attributable to the terephthalate moieties in Xydar or POB. This may be due to the predominance of the trans configuration of the two ester groups across the phenylene group, which has no net dipole moment, or due to the fact that rotations of the cis configuration are indistinguishable from those of the HBA dipoles.

Rheology. The most important aspect of the dynamic melt rheology data obtained for the POB S6635 copolymer is the frequency-independent behavior of the complex viscosity at frequencies below 1 rad/s; this result contrasts dynamic data obtained for other HBA-based copolymers (60/40 HBA/ET,^{17,25} 80/20 HBA/ET,²⁰ and 73/27 HBA/HNA^{23,24}) that display persistent shear-thinning behavior across this frequency range and that have characteristic complex viscosity-frequency curves that are concave upward. The frequency-independent behavior of the complex viscosity may be a reflection of the local interchain packing order that appears to be present in some parts of the POB melt at 370 °C (see Figures 3 and 4). It is difficult to draw any conclusions at this point as to possible "three-region" flow behavior for the POB, given the general lack of applicability of the Cox-Merz rule for these complex materials and the fundamental difference between steady and oscillatory shear;^{20,33} certainly steady-shear rheological measurements over a wide range of rates are in order for the POB material.

Consideration of the influence of shear history for the constant-temperature frequency sweeps shows that the material is very sensitive to prior shear within the time scale of the frequency progressions. Comparing the ascending and descending sweeps depicted in Figure 17, considerably reduced complex viscosity values are encountered for the sample exposed to a descending frequency progression; this behavior is a reflection of the shear-induced chain orientation that occurs at the higher frequencies. As the lowest frequencies are approached ($\omega \rightarrow 0.1$ rad/s) over the 5-min time scale of the experiment, the material relaxes, and the complex viscosity values approach those obtained during the ascending progression.

The frequency sweeps recorded with varying strain amplitudes indicate that the polymer behaves in a nonlinear fashion, particularly at higher frequencies (Figure 18); this result is not surprising, considering the complexity of the melt and the relatively high strain amplitudes imposed (10–100%). The reduction in the magnitude of the complex viscosity that is observed with increasing strain amplitude again appears to reflect the shear-induced chain orientation.

The cooling sweep that was recorded from the melt (Figure 19) indicates that below 350 °C, the material displays an essentially solidlike character, despite the high degree of local mobility that is evident in the dielectric

results over this temperature range; the dynamic rheological behavior is consistent with the hypothesis that the observed dielectric relaxations correspond to motions that are largely rotational, with very little translational motion. The source of the stepwise drop in moduli that appears at 275 °C upon cooling is not obvious; there is no clear transition in the thermal or X-ray data that explains this behavior. Efforts were made to reduce the possibility of experimental artifact (i.e., slippage), and the consistency and reproducibility of the data recorded at lower temperatures suggest that this was accomplished. Interestingly, rheological cooling sweeps performed on samples of Hoechst-Celanese Vectra A-900 (73/27 HBA/HNA) liquid crystalline copolymer displayed a similar stepwise drop in moduli, although at a somewhat lower temperature (~ 170 °C). (Another possibility besides slippage is that it might be an experimental artifact due to the data handling at very low loss angles.³⁴)

Conclusions

The structure and dynamics of two thermotropic liquid crystalline copolyesters based on 4-hydroxybenzoic acid and biphenol terephthalate have been investigated by X-ray diffraction, dielectric relaxation, and dynamic rheological techniques. The two commercial resins, Xydar SRT-300 and POB S6635, differ in the inclusion of a small fraction (4%) of isophthalic acid comonomer in the latter case, and the kinked structure of this randomly introduced constituent has a significant impact on the characteristics of the polymer. POB S6635, which has a processing temperature (ca. 360 °C) over 60 °C lower than that of Xydar SRT-300, shows a drastically reduced tendency to form three-dimensional ordered structures. The annealed sample exhibits a room temperature X-ray pattern resembling that of the PHBA homopolymer above ca. 340 °C (which is a smectic E type structure^{30,31}), but the 211 reflection is very weak and disappears by 300 °C, indicating predominantly hexagonal interchain packing. In contrast, the annealed Xydar sample displays a high degree of three-dimensional order (an orthorhombic cell) at room temperature. Around 100 °C the X-ray pattern changes to exhibit the features of the smectic E type PHBA, and above ca. 300 °C the 211 reflection disappears, indicating the predominance of hexagonal interchain packing order of highly extended chains at these high temperatures. Dielectric measurements, however, indicate the presence of rapid rotational mobility even in the most highly ordered structures of Xydar. Both materials display a low-temperature Arrhenius-type (β) relaxation which corresponds to localized motions of the HBA dipoles, and the POB copolymer displays an additional weak WLF-type (α) relaxation at higher temperatures which is due to motions involving the isophthalic acid groups. The relaxation strength observed for Xydar is consistent with a high degree of conformational order close to a 2_1 screw configuration along the chain axis, in close agreement with results obtained for the PHBA homopolymer above ca. 340 °C and for the HBA/HNA copolymers.¹⁴ In comparison, the POB copolymer exhibits a much larger relaxation strength across the β relaxation, indicating a lack of such conformational order. Dynamic rheological measurements, which were limited to the POB resin, indicate a shear-independent complex viscosity for the apparently nematic melt at low frequencies and a sensitivity to both shear history and strain amplitude. Rheological cooling sweeps were useful in determining the material solidification temperature and indicate an essentially temperature-independent solidlike behavior at temperatures below 350 °C, which seems to be dominated

by the rudimentary interchain packing order, despite the fact that the chain segments undergo rapid rotational motions at these temperatures.

Acknowledgment. We thank Norbert Niessner for the compositional analysis of the copolymers, Bruce Fuller for assistance with the dielectric measurements, and Norberto Masciocchi and Laura Depero for initial X-ray measurements on the Xydar SRT-300 samples.

References and Notes

- (1) IBM Visiting Scientist. Present address: Department of Chemical Engineering, University of Kentucky, Lexington, KY 40506.
- (2) IBM World Trade Visiting Scientist. Permanent address: Dipartimento di Fisica, Università di Salerno, I-84100 Salerno, Italy.
- (3) Economy, J. *Mol. Cryst. Liq. Cryst.* **1989**, *169*, 1.
- (4) Economy, J.; Cottis, S. G.; Nowak, B. E. U.S. Patents 3,637,595 (1972), 3,962,314 (1972), 3,772,250 (1973).
- (5) Jackson, W. J.; Kuhfuss, H. F. *J. Polym. Sci., Polym. Chem. Ed.* **1976**, *14*, 2043.
- (6) Calundann, G. W. U.S. Patents 4,161,407 (1979), 4,184,996 (1980).
- (7) Blackwell, J.; Cheng, H.-M.; Biswas, A. *Macromolecules* **1988**, *21*, 39.
- (8) Field, N. D.; Baldwin, R.; Layton, R.; Frayer, P.; Scardiglia, F. *Macromolecules* **1988**, *21*, 2155.
- (9) Cheng, S. Z. D.; Janimak, J. J.; Zhang, A.; Zhou, Z. *Macromolecules* **1989**, *22*, 4240.
- (10) Bechtoldt, H.; Wendorff, J. H.; Zimmermann, H. J. *Makromol. Chem.* **1987**, *188*, 651.
- (11) Blundell, D. J.; Buckingham, K. A. *Polymer* **1985**, *26*, 1623.
- (12) Takase, Y.; Mitchell, G. R.; Odajima, A. *Polym. Commun.* **1986**, *27*, 76.
- (13) Alhaj-Mohammed, M. H.; Davies, G. R.; Abdul Jawad, S.; Ward, I. M. *J. Polym. Sci., Polym. Phys. Ed.* **1988**, *26*, 1751.
- (14) Kalika, D. S.; Yoon, D. Y. *Macromolecules*, preceding paper in this issue.
- (15) Gedde, U. W.; Buerger, D.; Boyd, R. H. *Macromolecules* **1987**, *20*, 988.
- (16) Nicely, V. A.; Dougherty, J. T.; Renfro, L. W. *Macromolecules* **1987**, *20*, 573.
- (17) Amundson, K. R.; Kalika, D. S.; Shen, M.-R.; Yu, X.-M.; Denn, M. M.; Reimer, J. A. *Mol. Cryst. Liq. Cryst.* **1987**, *153*, 271.
- (18) Asada, S.; Onogi, T. In *Rheology Principles*; Astarita, G., Marrucci, G., Nicolais, L., Eds.; Plenum: New York, 1980; Vol. I.
- (19) Wissbrun, K. F. *J. Rheol.* **1981**, *25*, 619.
- (20) Kalika, D. S.; Giles, D. W.; Denn, M. M. *J. Rheol.* **1990**, *34*, 139.
- (21) Jerman, R. E.; Baird, D. G. *J. Rheol.* **1981**, *25*, 275.
- (22) Gotsis, A. D.; Baird, D. G. *J. Rheol.* **1985**, *29*, 539.
- (23) Wissbrun, K. F.; Kiss, G.; Cogswell, F. N. *Chem. Eng. Commun.* **1987**, *53*, 149.
- (24) Kalika, D. S.; Nuel, L.; Denn, M. M. *J. Rheol.* **1989**, *33*, 1059.
- (25) Wissbrun, K. F. *Br. Polym. J.* Dec 1980, 161.
- (26) Niessner, N.; Johnson, R. D.; Lyerla, J. R., in preparation.
- (27) Dartco Mfg., Inc. *Xydar Technical Information*, 1985.
- (28) Sumitomo Chemical Co., Ltd. *Super Heat Resistant Injection Molding Material: POB*, 1989.
- (29) Kalika, D. S.; Shen, M.-R.; Yu, X.-M.; Denn, M. M.; Iannelli, P.; Masciocchi, N.; Yoon, D. Y.; Parrish, W.; Friedrich, C.; Noël, C. *Macromolecules* **1990**, *23*, 5192.
- (30) Yoon, D. Y.; Masciocchi, N.; Depero, L.; Viney, C.; Parrish, W. *Macromolecules* **1990**, *23*, 1793.
- (31) Coulter, P. D.; Hanna, S.; Windle, A. H. *Liq. Cryst.* **1989**, *5*, 1603.
- (32) Kricheldorf, H. R.; Schwarz, G. *Polymer* **1990**, *31*, 481.
- (33) Cox, W. P.; Merz, E. H. *J. Polym. Sci.* **1958**, *28*, 619.
- (34) Wissbrun, K. F., personal communication.

Registry No. Xydar SRT-300, 31072-56-7; POBS6635, 60088-52-0.